Novel Aromatic Polyamides and Polyimides Functionalized with 4-*tert*-Butyltriphenylamine Groups

SHENG-HUEI HSIAO,[1] YU-MIN CHANG,[1] HWEI-WEN CHEN,[2] GUEY-SHENG LIOU[2]

[1]Department of Chemical Engineering, Tatung University, 40 Chungshan North Road, 3rd Section, Taipei 104, Taiwan, Republic of China

[2]Department of Applied Chemistry, National Chi Nan University, 1 University Road, Puli, Nantou Hsien 545, Taiwan, Republic of China

ABSTRACT: A new triphenylamine-containing diamine monomer, 4,4′-diamino-4″-*tert*-butyltriphenylamine, was successfully synthesized by the cesium fluoride-mediated *N,N*-diarylation of 4-*tert*-butylaniline with 4-fluoronitrobenzene, followed by the reduction of the nitro group. The obtained diamine monomer was reacted with various aromatic dicarboxylic acids and tetracarboxylic dianhydrides to produce two series of novel triphenylamine-based polyamides and polyimides with pendent *tert*-butyl substituents. Most of the polymers were readily soluble in polar organic solvents, such as *N*-methyl-2-pyrrolidone and *N,N*-dimethylacetamide (DMAc), and could be solution cast into tough and flexible polymer films. These polymers showed high glass transition temperatures between 282 and 320 °C, and they were fairly stable up to a temperature above 450 °C (for polyamides) or 500 °C (for polyimides). These polymers exhibited UV absorption maxima around 308 to 361 nm. The photoluminescence spectra of the polyamides in DMAc exhibited a peak emission wavelength in the blue at 421–433 nm. Cyclic voltammograms of polyamides and polyimides showed an oxidation wave at 1.0–1.1 V versus Ag/AgCl in an acetonitrile solution. All the polyamides and polyimides exhibited excellent reversibility of electrochromic characteristics by continuous several cyclic scans between 0.0 and 1.1–1.3 V, with a color change from the original pale yellowish neutral form to the green or blue oxidized forms. © 2006 Wiley Periodicals, Inc. J Polym Sci Part A: Polym Chem 44: 4579–4592, 2006

Keywords: electrochemistry; electrochromism; luminescence; polyamides; polyimides; triphenylamine

INTRODUCTION

Aromatic polyamides and polyimides constantly attract interest because they exhibit excellent thermal, mechanical, and electrical properties as well as outstanding chemical resistance.[1–4] However, most of them have high melting or softening temperature (T_s) and are insoluble in most of organic solvents partly because of the strong interchain interaction. These properties make them generally intractable or difficult to process, thus limiting their applications. To overcome these limitations, many efforts have been made to improve the processing characteristics of these intractable polymers while other advantageous properties are retained.[5–8] Different structural modifications of the polymer backbone have been studied to reduce the chain–chain

interaction, for example, the incorporation of bulky, packing-disruptive moieties, which hinder the chain packing but do not affect the glass transition temperature.[9–21] It has been demonstrated that aromatic polyamides and polyimides containing bulky, propeller-shaped triphenylamine unit were amorphous, had excellent or enhanced solubility in organic solvents, and exhibited high thermal stability.[22–27] Recently, we further studied the optoelectronic properties of triphenylamine-based polyamides, polyimides, polyhydrazides, and polyoxadiazoles and found that these polymers exhibited stable photoluminscent and electrochromic characteristics in addition to good film-forming capability and high thermal stability.[28–31]

The anodic oxidation of triphenylamine in aprotic solvent is well studied.[32] The one-electron oxidation product, triphenylamine radical cation, is not stable. The chemical follow-up reaction produces tetraphenylbenzidine by tail-to-tail (para positions) coupling, with the loss of two protons per dimer. When the phenyl groups are substituted at the para position, the coupling reactions are greatly prevented. It has been well established that incorporation of electron-donating substitutents at the para position of triarylamines affords stable radical cations.[33,34] Therefore, we synthesized the diamine monomer, 4,4′-diamino-4″-*tert*-butyltriphenylamine (**2**), and its derived polyamides and polyimides containing electron-rich triphenylamine groups with *tert*-butyl para substituted on the pendent phenyl ring. We particularly targeted electron-donating para substituent that lacks benzylic hydrogens. Thus, this design obviates not only dimerization pathways through the para position, but also the possible dimerization through a benzylic position. The *tert*-butyl groups are expected to increase the solubility of the polymers and provide stability to the triphenylamine in its oxidized form.

EXPERIMENTAL

Materials

4-*tert*-Butylaniline (Acros), 4-fluoronitrobenzene (Acros), 10% palladium on charcoal (Pd/C) (Fluka), cesium fluoride (CsF) (Acros), triphenyl phosphite (TPP) (TCI), and hydrazine monohydrate (Acros) were used without further purification. *N,N*-Dimethylacetamide (DMAc) (Fluka), *N,N*-dimethylformamide (Acros), pyridine (Wako),

and *N*-methyl-2-pyrrolidone (NMP) (Fluka) were dried over calcium hydride overnight, distilled under reduced pressure, and stored over 4 Å molecular sieves in a sealed bottle. The commercially available aromatic dicarboxylic acids such as terephthalic acid (**3a**) (Wako), isophthalic acid (**3b**) (Wako), 4,4′-biphenydicarboxylic acid (**3c**) (TCI), 4,4′-dicarboxydiphenyl ether (**3d**) (TCI), bis(4-carboxyphenyl) sulfone (**3e**) (New Japan Chemicals), 2,2-bis(4-carboxyphenyl)hexafluoropropane (**3f**) (TCI), 1,4-naphthalenedicarboxylic acid (**3g**) (Wako), 2,6-naphthalenedicarboxylic acid (**3h**) (TCI) were used as received. Commercially obtained calcium chloride was dried under vacuum at 150 °C for 6 h prior to use. Commercially available aromatic tetracarboxylic dianhydrides such as pyromellitic dianhydride (**5a**) (Aldrich) and 3,3′,4,4′-benzophenonetetracarboxylic dianhydride (BTDA; **5c**) (Aldrich) were purified by recrystallization from acetic anhydride. 3,3′,4,4′-Biphenyltetracarboxylic dianhydride (**5b**) (Oxychem), 4,4′-oxydiphthalic dianhydride (ODPA; **5d**) (Oxychem), 3,3′,4,4′-diphenylsulfonetetracarboxylic dianhydride (**5e**) (New Japan Chemical), and 2,2-bis(3,4-dicarboxyphenyl)hexafluoropropane dianhydride (6FDA; **5f**) (Hoechst Celanese) were heated at 250 °C *in vacuo* for 3 h before use.

Monomer Synthesis

4-tert-*Butyl-4′,4″-dinitrotriphenylamine (1)*

In a 250 mL round-bottom flask equipped with a stirring bar, a mixture of 14.9 g (0.1 mol) of 4-*tert*-butylaniline, 28.6 g (0.2 mol) of 4-fluoronitrobenzene, and 30.4 g (0.2 mol) of CsF in 100 mL of dimethyl sulfoxide (DMSO) was heated with stirring at 140 °C for 12 h. After cooling, the mixture was poured into 300 mL of water, and the precipitate was collected by filtration and washed thoroughly with water. Recrystallization from methanol yielded 23.8 g of the desired dinitro compound **1** as yellow crystals in 63% yield [mp = 144–145 °C, measured by differential scanning calorimetry (DSC) at a scan rate of 2 °C/min].

Infrared (IR) (KBr): 1581, 1340 cm^{-1} (—NO$_2$ stretch). ^{1}H-NMR (500 MHz, DMSO-d$_6$, δ, ppm): 8.18 (d, J = 9.1 Hz, 4H, H$_a$), 7.53 (d, J = 8.5 Hz, 2H, H$_d$), 7.19 (two overlapped doublets, 6H, H$_b$ + H$_c$), 1.32 (s, 9H, *t*-butyl). ^{13}C-NMR (125 MHz, DMSO-d$_6$, δ, ppm): 151.59 (C^7), 149.61 (C^1), 141.88 (C^{10}), 141.68 (C^4), 127.30 (C^3), 126.83 (C^2), 125.50 (C^9), 122.20 (C^8), 34.33 (C^5), 30.99 (C^6).
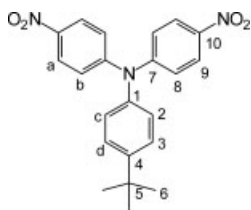
4,4′-Diamino-4″-tert-*butyltriphenylamine (2)*

In a 300 mL round-bottom flask, 19.6 g (0.05 mol) of dinitro compound **1**, 0.2 g of 10 wt % Pd/C, 10 mL of hydrazine monohydrate, and 100 mL of ethanol was heated at a reflux temperature for 12 h. The solution was filtered hot to remove Pd/C. After cooling, the mixture was poured into 400 mL of water, and the next day the precipitate was collected by filtration, and then dried in vacuum to afford 13.4 g (80% yield) of diamine **2** as pale purple powder. The crude product could be further purified by recrystallization from ethanol under nitrogen as pale gray needles; mp = 113–115 °C (DSC, 2 °C/min).

IR (KBr): 3407, 3324 cm^{-1} (N—H stretch). ^{1}H-NMR (500 MHz, DMSO-d$_6$, δ, ppm): 7.09 (d, J = 8.5 Hz, 2H, H$_d$), 6.79 (d, J = 8.5 Hz, 4H, H$_b$), 6.63 (d, J = 8.5 Hz, 2H, H$_c$), 6.57 (d, J = 8.5 Hz, 4H, H$_a$), 4.88 (s, 4H, —NH$_2$), 1.21 (s, 9H, *t*-butyl). ^{13}C-NMR (125 MHz, DMSO-d$_6$, δ, ppm): 147.15 (C^1), 145.04 (C^{10}), 140.65 (C^4), 137.01 (C^7), 127.01 (C^8), 125.51 (C^3), 117.55 (C^2), 115.22 (C^9), 33.73 (C^5), 31.53 (C^6). ANAL. Calcd for C$_{22}$H$_{25}$N$_3$ (331.46): C, 79.72%; H, 7.60%; N, 12.68%. Found: C, 79.05%; H, 7.83%; N, 12.66%.
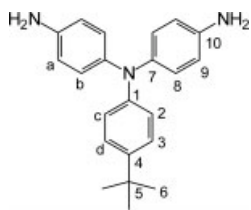
Polymer Synthesis

Synthesis of Polyamides

The synthesis of polyamide **4a** is used as an example to illustrate the general synthetic route used to produce the polyamides. A 50 mL round-bottom flask equipped with a magnetic stirrer was charged with 0.4872 g (1.50 mmol) of diamine momomer **2**, 0.2492 g (1.50 mmol) of terephthalic acid (**3a**), 1.5 mL of TPP, 4 mL of NMP, 0.5 mL of

pyridine, and 0.2 g of calcium chloride. The reaction mixture was heated with stirring at 110 °C for 3 h. The resulting viscous polymer solution was poured slowly into 300 mL of stirring methanol giving rise to a stringy, fiber-like precipitate that was collected by filtration, washed thoroughly with hot water and methanol, and dried. The inherent viscosity of the resulting polyamide **4a** was 0.97 dL/g, measured in DMAc at a concentration of 0.5 g/dL at 30 °C. The IR spectrum of **4a** (film) exhibited characteristic amide absorption bands at 3303 (amide N—H stretch) and 1653 cm^{-1} (amide C=O stretch).

Synthesis of Polyimides

A typical procedure is as follows. The diamine monomer **2** (0.5070 g, 1.530 mmol) was dissolved in 9.5 mL of DMAc in a 50-mL round-bottom flask. Then BTDA (0.4929 g, 1.530 mmol) was added to the diamine solution in one portion. Thus, the solid content of the solution is approximately 10 wt %. The mixture was stirred at room temperature for about 3 h to yield a viscous poly (amic acid) solution. The inherent viscosity of the resulting poly(amic acid) was 1.55 dL/g, measured in DMAc at a concentration of 0.5 g/dL at 30 °C. The poly(amic acid) film was obtained by casting from the reaction polymer solution onto a glass Petri dish and drying at 90 °C overnight. The poly(amic acid) in the form of film was converted to polyimide **6c** by successive heating under vacuum at 150 °C for 30 min, 200 °C for 30 min, and then 250 °C for 1 h. The inherent viscosity of polyimide **6c** was 0.44 dL/g, measured at a concentration of 0.5 g/dL in concentrated sulfuric acid at 30 °C. The IR spectrum of **6c** (film) exhibited characteristic imide absorption bands at 1778 (asymetrical C=O stretch), 1724 (symmetrical C—O stretch), and 1376 cm^{-1} (C—N stretch).

For the chemical imidization method, 5 mL of acetic anhydride and 2 mL of pyridine were added to the poly(amic acid) solution obtained by a similar process as above, and the mixture was heated at 100 °C for 1 h to effect a complete imidization. The resulting reddish precipitate was washed thoroughly with methanol and water, collected by filtration, and dried at 150 °C for 4 h.

Preparation of the Polyamide Films

A polymer solution was made by the dissolution of about 0.7 g of the polyamide sample in 10 mL of hot DMAc. The homogeneous solution was poured

into a 7-cm glass Petri dish, which was placed in a 90 °C oven overnight for the slow release of the solvent, and then the film was stripped off from the glass substrate and further dried in vacuum at 160 °C for 6 h. The obtained films were about 90 μm thick and were used for X-ray diffraction measurements, tensile tests, solubility tests, and thermal analyses.

Measurements

IR spectra were recorded on a Horiba FT-720 Fourier transform infrared (FTIR) spectrometer. Elemental analyses were run in a Heraeus VarioEL-III CHN elemental analyzer. ^{1}H and ^{13}C-NMR spectra were measured on a Bruker AVANCE 500 FT-NMR system with tetramethylsilane as an internal standard. The inherent viscosities were determined with an Ubbelohde or a Cannon-Fenske viscometer at 30 °C. Wide-angle X-ray diffraction measurements were performed at room temperature (~25 °C) on a Shimadzu XRD-6000 X-ray diffractometer with a graphite monochromator (operating at 40 kV and 30 mA), using nickel-filtered Cu–Kα radiation [$\lambda = 1.5418$ Å (Angstrom)]. The scanning rate was 2°/min over a range of $2\theta = 10$–$40°$. Ultraviolet-visible (UV–vis) spectra of the polymer films were recorded on a Jasco UV/VIS V530 spectrometer. A universal tester LLOYD LRX with a load cell 5 kg was used to study the stress–strain behavior of the samples. A gauge length of 2 cm and a crosshead speed of 5 mm/min were used for this study. Measurements were performed at room temperature with film specimens (0.5 cm width, 6 cm length), and an average of three to five replicates were used. Thermogravimetric analysis (TGA) was performed with a PerkinElmer Pyris 1 TGA. Experiments were carried out on approximately 4–6 mg of samples heated in flowing nitrogen or air (flow rate = 40 cm^3/min) at a heating rate of 20 °C/min. DSC analyses were performed on a PerkinElmer Pyris 1 DSC at a scan rate of 20 °C/min in flowing nitrogen. Thermomechanical analysis (TMA) was determined with a PerkinElmer TMA 7 instrument. The TMA experiments were carried out from 50 to 350 °C at a scan rate of 10 °C/min with a penetration probe 1.0 mm in diameter under an applied constant load of 10 mN. T_s were taken as the onset temperatures of probe displacement on the TMA traces. Electrochemistry was performed with a Bioanalytical System Model CV-27 potentiostat and a BAS X–Y recorder. Voltammograms are presented with the positive potential pointing to the left and with increasing anodic currents pointing downwards. Cyclic voltammetry was conducted with the use of a three-electrode cell in which ITO (polymer films area about 0.7 cm × 0.5 cm) was used as a working electrode. A platinum wire was used as an auxiliary electrode. All cell potentials were taken with the use of a home-made Ag/AgCl, KCl (sat.) reference electrode. Ferrocene was used as an external reference for calibration (+0.44 V versus Ag/AgCl). Spectroelectrochemistry analyses were carried out with an electrolytic cell, which was composed of a 1 cm cuvette, ITO as a working electrode, a platinum wire as an auxiliary electrode, and a Ag/AgCl reference electrode. Absorption spectra were measured with a HP 8453 UV–vis spectrophotometer. Photoluminescence (PL) spectra were measured with a Varian Cary Eclipse fluorescence spectrophotometer.

RESULTS AND DISCUSSION

Monomer Synthesis

4,4′-Diamino-4″-*tert*-butyltriphenylamine (**2**) was prepared by the double *N*-arylation of 4-*tert*-butylaniline with 4-fluoronitrobenzene, followed by hydrazine Pd/C-catalytic reduction of the intermediate dinitro compound **1** according to the synthetic route outlined in Scheme 1. Elemental analysis, IR, and ^{1}H and ^{13}C-NMR spectroscopic techniques were used to identify the structures of the intermediate compound **1** and the targeted diamine monomer **2**. The ^{1}H-NMR and ^{13}C-NMR spectra of the diamine monomer **2** are illustrated in Figure 1. Assignments of each carbon and proton are also given in these figures, and these spectra agree well with the proposed molecular structure of **2**. The ^{1}H-NMR spectra confirm that the nitro groups have been completely transformed into the amino groups by the high field shift of the aromatic protons and by the resonance signals at around 4.8 ppm corresponding to the amino protons. The resonance signals appeared at 1.2–1.3 ppm in the ^{1}H-NMR spectra and 34 ppm (quaternary carbons) and 31 ppm (primary carbons) in the ^{13}C-NMR spectra are peculiar to the *tert*-butyl group.

Polymer Synthesis

As shown in Scheme 2, polyamides **4a–4h** were prepared from the diamine **2** with various aromatic dicarboxylic acids (**3a–3h**) in NMP containing
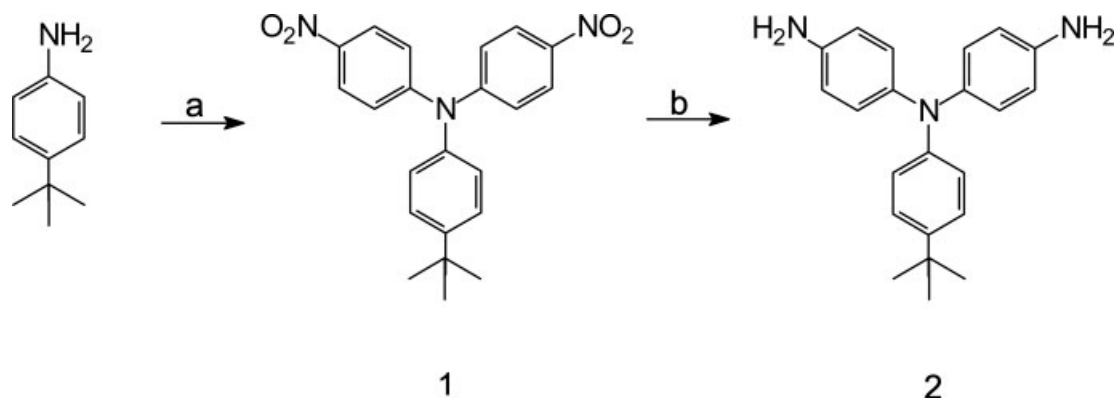
Scheme 1. Synthetic route to the target diamine monomer **2.** (a) 4-Fluoronitrobenzene, DMSO, CsF, 120 °C, (b) Ethanol, $NH_2NH_2 \cdot H_2O$, Pd/C, reflux.

dissolved calcium chloride by the Yamazaki–Higashi reaction conditions[35] using TPP and pyridine as condensing agents. All polyamides remained soluble in the reaction medium, thus permitting an increase of their molecular weight and giving highly viscous solutions. The polyamides were produced with moderate to high inherent viscosities ranging from 0.44 to 1.21 dL/g (Table 1). The molecular weights of all the polyamides are sufficiently high to permit the formation of flexible and tough films by casting from

their DMAc solutions. Structural features of these polyamides were confirmed by FTIR spectroscopy. They exhibited characteristic absorptions of the amide group around 3300 (N—H stretching) and 1650 cm^{-1} (C=O stretching). A typical FTIR spectrum of polyamide **4a** is shown in Figure 2(a).

Polyimides **6a–6f** were prepared in conventional two-step method by the reactions of equal molar amounts of diamine **2** with various aromatic dianhydrides (**5a–5f**) to form poly(amic
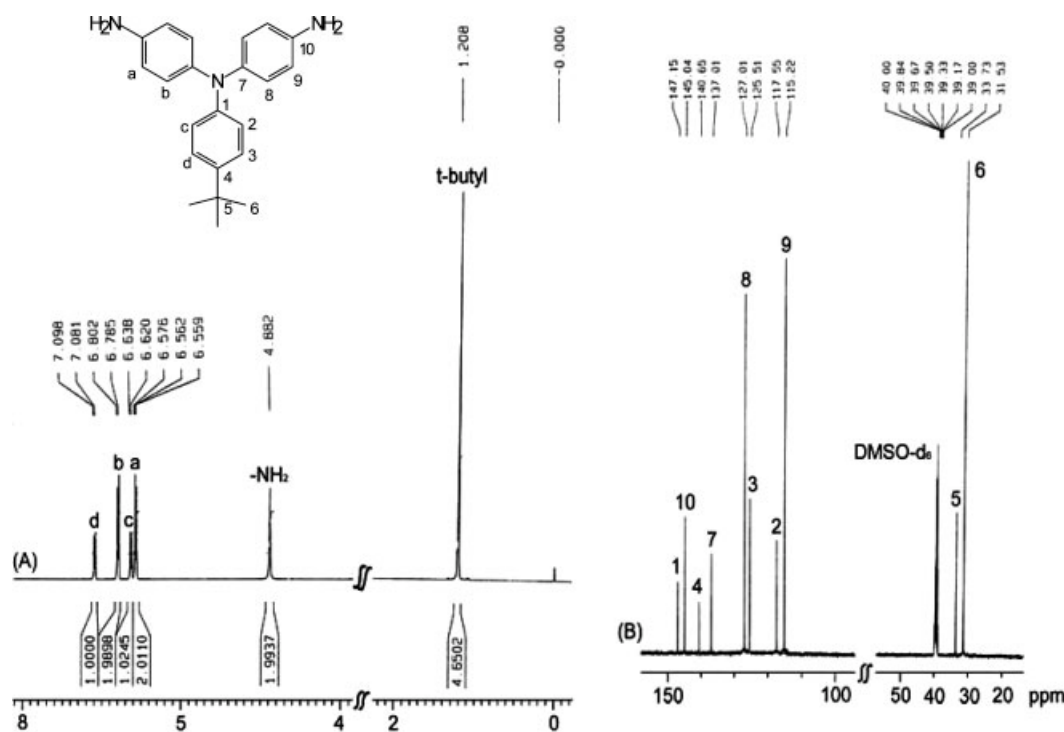
Figure 1. (a) ^{1}H-NMR spectrum and (b) ^{13}C-NMR spectrum of 4,4′-diamino-4″-*tert*-butyltriphenylamine (**2**) in DMSO-d_6.

Scheme 2. Synthesis of polyamides.
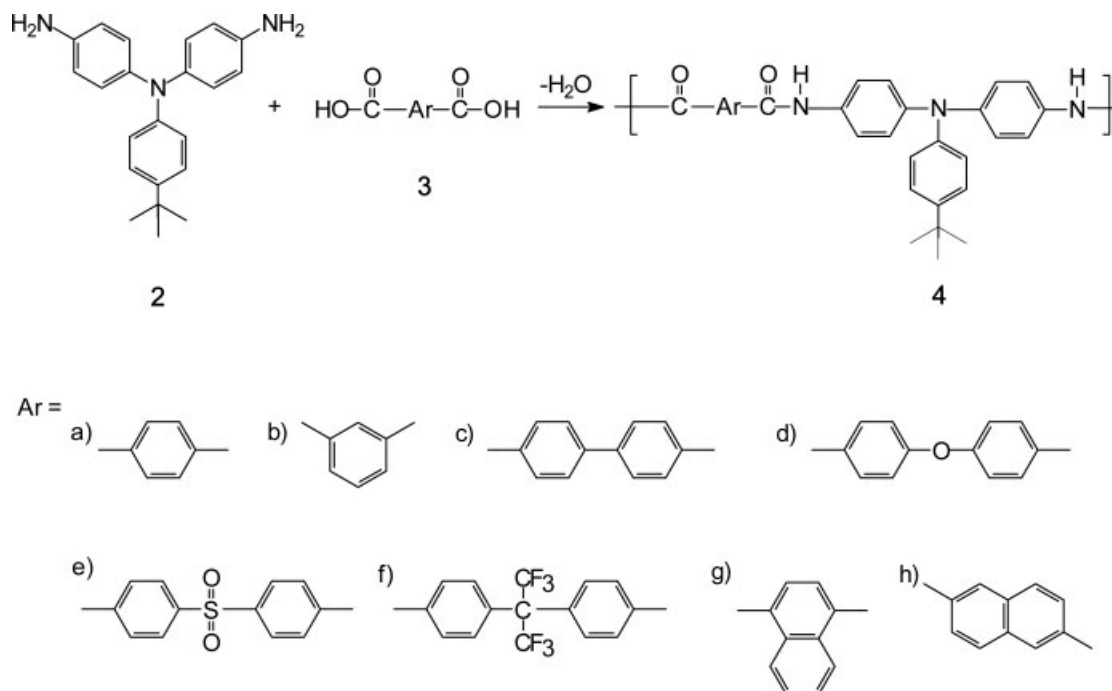
acid)s, followed by thermal or chemical cyclodehydration (Scheme 3). As shown in Table 2, the inherent viscosities of the poly(amic acid) precursors were in the range 1.15–2.02 dL/g, indicating the formation of high-molecular-weight polymers. All of these poly(amic acid)s could be solution cast into flexible and tough films, which were subsequently converted into tough polyimide films by extended heating at elevated temperatures. The poly(amic acid)s also could be chemically cyclodehydrated to polyimides by treatment with a mixture of pyridine and acetic anhydride. The complete imidization of polymers was confirmed by IR spectra. All the polyimides showed the characteristic absorption bands of the imide ring near 1780 (asymmetric C=O stretch), 1720 (symmetric C=O stretch), 1380 (C—N stretch), and 720 cm^{-1} (imide ring deformation). A representative IR spectrum for polyimide **6c** is illustrated in Figure 2(b). There was no existence of the characteristic absorption bands of the amide groups near 3300 (N—H stretch) and 1650 (C=O stretch) cm^{-1},

Table 1. Inherent Viscosity and Solubility Behavior of Polyamides

Polymer Code	η_{inh}[a] (dL/g)	Solubility in Various Solvents[b]					
		NMP	DMF	DMAc	DMSO	m-Cresol	THF
4a	0.97	+	+	+	+h	+h	−
4b	0.44	+	+	+	+	+	−
4c	1.21	+	+	+	−	+h	−
4d	0.95	+	+	+	+	+	−
4e	0.82	+	+	+	+	+	−
4f	0.62	+	+	+	+h	+	+
4g	0.96	+	−	+	−	+h	−
4h	1.15	+	+	+	−	+h	−

[a] Measured at a concentration of 0.5 g/dL in DMAc containing 5 wt % LiCl at 30 °C.
[b] Qualitative solubility was tested with 10 mg of a sample in 1 mL of stirred solvent.
NMP, N-methyl-2-pyrrolidone; DMAc, N,N-dimethylacetamide; DMF, N,N-dimethylformamide; DMSO, dimethyl sulfoxide; THF, tetrahydrofuran.
+, soluble at room temperature; +h, soluble on heating; −, insoluble even on heating.
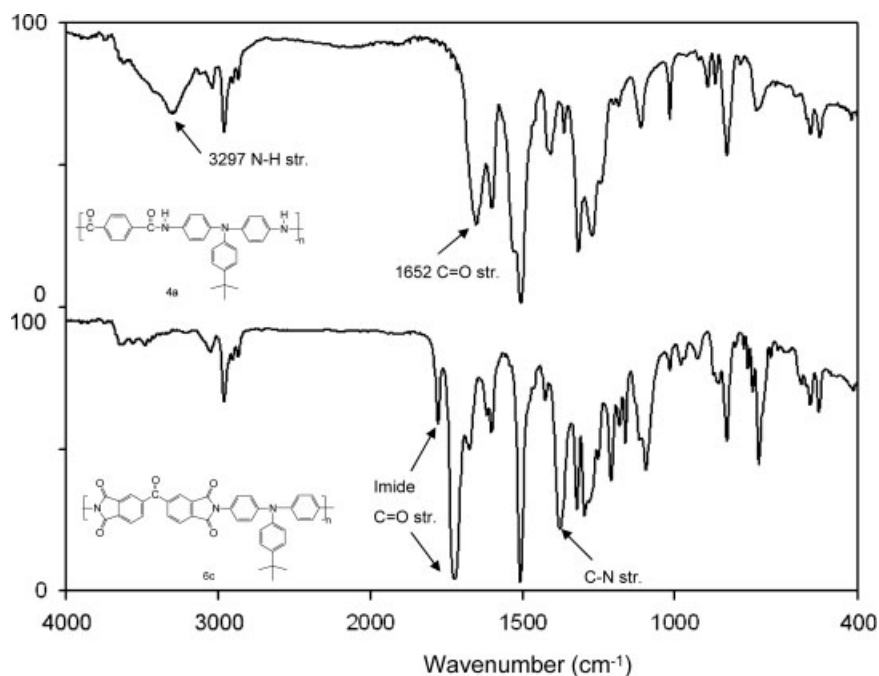
Figure 2.   Thin film IR spectra of (a) polyamide **4a** and (b) polyimide **6c**.

indicating that polymers had been fully imidized. These thermally or chemically imidized polyimides exhibited inherent viscosities between 0.29 and 0.76 dL/g. The organosoluble ones such as **6d–6f** could be solution cast into strong films in the fully imidized form.

Polymer Properties

Solubility and Film Property

The solubility behavior of the polyamides and polyimides in several organic solvents at 10% (w/v) is summarized in Tables 1 and 2, respectively. Except
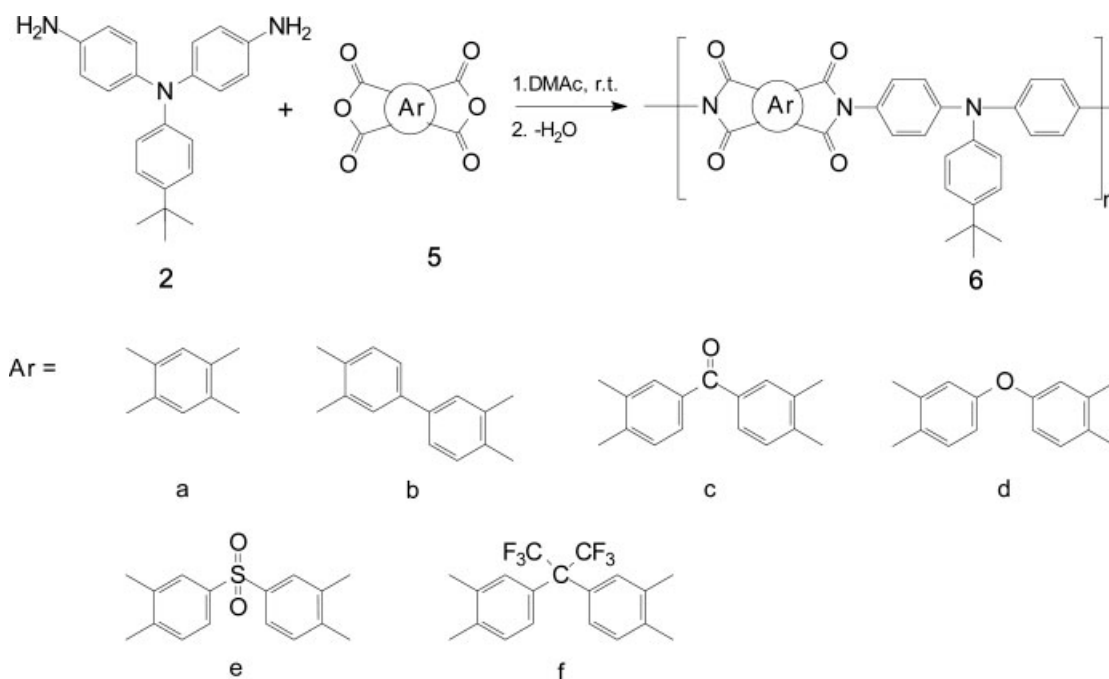
Scheme 3.   Synthesis of polyimides.

Table 2. Inherent Viscosity and Solubility Behavior of Polyimides Prepared via Thermal (−T) or Chemical (−C) Imidization

| Polymer | η_{inh} (dL/g) | | Solubility in Various Solvents[a] | | | | | |
	Poly(amic acid)[b]	Polyimide[c]	NMP	DMAc	DMF	DMSO	m-Cresol	THF
6a-T	1.75	0.29	−	−	−	−	−	−
6a-C	−	−[d]	−	−	−	−	−	−
6b-T	2.02	0.43	−	−	−	−	−	−
6b-C	−	0.36	−	−	−	−	+	−
6c-T	1.55	−[d]	−	−	−	−	−	−
6c-C	−	0.44	+h	−	−	−	+h	−
6d-T	1.74	0.76	−	+h	−	−	+h	−
6d-C	−	0.53 (0.32)[b]	+	+	−	−	+	+
6e-T	1.25	0.49 (0.36)	+	+	+	−	+h	−
6e-C	−	0.76 (0.71)	+	+	+	−	+h	+h
6f-T	1.15	0.29 (0.36)	+	+	+	−	+h	+
6f-C	−	0.70 (0.72)	+	+	+	−	+h	+

[a] Qualitative solubility was tested with 10 mg of a sample in 1 mL of stirred solvent.
[b] Measured at a concentration of 0.5 g/dL in DMAc at 30 °C.
[c] Measured at a concentration of 0.5 g/dL in conc. H_2SO_4 at 30 °C.
[d] Insoluble in conc. H_2SO_4 and polar organic solvents.
NMP, N-methyl-2-pyrrolidone; DMAc, N,N-dimethylacetamide; DMF, N,N-dimethylformamide; DMSO, dimethyl sulfoxide; THF, tetrahydrofuran.
+, soluble at room temperature; +h, soluble on heating; −, insoluble even on heating.

for the polyimides derived from more rigid dianhydrides such as **6a–6c**, the other polyimides and almost all polyamides exhibited good solubility in a variety of solvents such as NMP, DMAc, N,N-dimethylformamide, and DMSO at room temperature or upon heating at 70 °C. In general, these polymers revealed an enhanced solubility as compared with conventional aromatic polyamides and polyimides. This can be attributed in part to the incorporation of bulky, three-dimensional *tert*-butyltriphenylamino groups, which retard dense chain packing and lead to a decreased chain–chain interaction. Therefore, the good solubility makes these polymers potential candidates for practical applications in spin-coating and inkjet-printing processes. All of the polymers could afford flexible and tough films, and they were amorphous in nature as evidenced by wide-angle X-ray diffraction patterns. These films exhibited good mechanical properties with tensile strengths of 52–103 MPa, elongations at break of 3–22%, and tensile moduli of 1.5–2.3 GPa. Most of the polymer films exhibited high tensile strengths and moderate elongation to break; thus, they could be considered as strong and ductile materials.

Thermal Properties

For the creation of useful devices based on organic light-emitting or charge-transporting materials, stable and high-quality amorphous glassy materials are required. TGA, DSC, and TMA were used to investigate the thermal properties of the polyamides and polyimides. The thermal behavior data of all the polymers are summarized in Table 3. The polyamides showed T_g values between 282 and 302 °C. The lowest T_g value of **4b** can be explained in terms of the flexibility and low rotation barrier of its diacid moiety. For comparison, previously reported[29] T_g values of the corresponding polyamides (**4′**) without the *tert*-butyl substituent are also listed in Table 4. In most cases, the **4** series polyamides showed comparable T_g values to those of the corresponding **4′** ones. This result indicated that the increased mobility hindrance of the pendent *tert*-butyl groups was balanced by the effects of increased free volume and decreased interchain interactions introduced with the pendent groups. The T_s (may be referred as apparent T_g) of the polyamide films were determined by the TMA method using a loaded penetration probe. They were read from the onset temperature of the probe displacement on the TMA trace. The T_s values measured by TMA are also listed in Table 3. As can be seen, in all cases, the T_s values of the polyamides obtained by TMA are lower than the T_g values measured by the DSC experiments. These differences may be attributed to the different heating story of the samples and the distinct nature of these two testing

Table 3. Thermal Properties of Polyamides and Polyimides[a]

Polymer Code	T_g[b] (°C)	T_s[c] (°C)	T_d[d] (°C)		Char Yield[e] (wt %)
			In N$_2$	In Air	
4a	295 (295)[f]	290 (298)[f]	495 (546)[f]	494 (526)[f]	67
4b	282 (290)	272 (271)	487 (554)	472 (513)	65
4c	294 (302)	281 (305)	484 (573)	476 (528)	63
4d	286 (273)	276 (269)	481 (581)	471 (523)	66
4e	302 (296)	290 (292)	468 (515)	465 (504)	63
4f	298 (295)	282 (302)	498 (544)	491 (525)	60
4g	286 (288)	275 (292)	458 (564)	451 (532)	62
4h	295 (307)	286 (315)	489 (569)	481 (535)	68
6a	314 (−)	292 (314)	563 (606)	559 (596)	69
6b	319 (331)	308 (314)	581 (613)	567 (619)	69
6c	294 (309)	292 (290)	556 (590)	553 (590)	61
6d	289 (295)	283 (292)	569 (608)	565 (611)	64
6e	320 (326)	298 (291)	524 (546)	518 (577)	53
6f	301 (316)	295 (310)	561 (581)	548 (571)	61

[a] The polymer film sample were heated at 300 °C for 1 h prior to all the thermal analyses.
[b] Midpoint temperature of baseline shift on the heating DSC trace (from 30 to 400 °C at 20 °C/min).
[c] Softening temperature taken as the onset temperature of the probe displacement on the TMA trace at a heating rate of 10 °C/min.
[d] Decomposition temperature at which a 10 wt % loss was recorded by TGA at a heating rate of 20 °C/min and a gas flow rate of 30 cm^3/min.
[e] Residual weight percent at 800 °C in nitrogen.
[f] Values in parentheses are data of analogous polyamides (**4′**) and polyimides (**6′**) having the corresponding Ar as that of the **4** and **6** series.
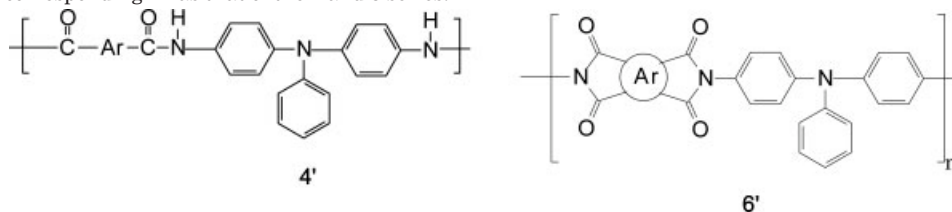
methods. As shown in Table 3, polyamides **4a–4h** showed decomposition temperatures (T_d) at which a 10% weight loss was recorded in the ranges of 458–498 °C in nitrogen and 451–494 °C in air, with more than 60% residue remaining when they were heated to 800 °C in nitrogen. All the **4** series polyamides exhibited a lower T_d value as compared with their corresponding counterparts without the *tert*-butyl group. This is reasonable when considering the less stable aliphatic segments.

The thermal behavior data of polyimides **6a–6f** together with their referenced analogs (**6a′–6f′**) are also included in Table 3. The T_g values of the **6a–6f** series polyimides measured by DSC were recorded in the range 289–320 °C. The decreasing order of T_g generally correlated with that of chain flexibility. For example, the polyimide **6d** from ODPA showed the lowest T_g (289 °C) because of the presence of flexible ether linkage between the phthalimide units. The **6** series polyimides showed slightly lower T_g values as compared with their counterpart **6′** series without the *tert*-butyl substituent. This might be a result of reduced chain-to-chain interaction and packing because of the bulky pendent groups. The **6** series polyimides exhibited T_s values of 283–308 °C, which were comparable with or slightly lower than those of the **6′** series. The T_ds at 10% weight loss of the polyimides (**6a–6f**) in nitrogen and air remained in the range of 524–581 °C and 518–567 °C, respectively. They left more than 53% char yield at 800 °C in nitrogen. Slightly lower T_ds for polyimides **6a–6f** as compared with **6a′–6f′** also could be ascribed to the introduction of *tert*-butyl groups.

Optical and Electrochemical Properties

The optical and electrochemical properties of these polymers were investigated by UV–vis and PL spectroscopy and cyclic voltammetry. The

Table 4. Optical and Electrochemical Properties of Polyamides and Polyimides

Polymer Code	$\lambda_{abs, max}$ (nm)[a]	$\lambda_{abs, onset}$ (nm)[b]	λ_{PL} (nm)[a]	$E_{1/2}$ (V)[c] (vs. Ag/Ag$^+$)	E_g[d] (eV)	HOMO[e] (eV)	LUMO[f] (eV)
4a	346	441	430	0.82	2.81	5.18	2.37
4b	341	404	424	0.84	3.07	5.20	2.13
4c	286, 361	426	422	0.81	2.91	5.17	2.26
4d	336	394	427	0.82	3.15	5.18	2.03
4e	280, 361	443	421	0.85	2.80	5.21	2.41
4f	312, 356	415	425	0.85	2.99	5.21	2.22
4g	314	402	425	0.85	3.08	5.21	2.13
4h	300, 361	434	421	0.80	2.86	5.16	2.30
4a$'$	317	388	437	0.85	3.19	5.21	2.02
4c$'$	297, 354	420	440	0.86	2.95	5.22	2.27
4d$'$	338	382	433	0.85	3.25	5.21	1.96
4e$'$	298, 381	429	429	0.87	2.89	5.27	2.38
6c	309	397	–	1.09	3.12	5.45	2.33
6d	317	383	–	1.08	3.24	5.44	2.20
6e	304	380	–	1.09	3.26	5.45	2.19
6f	303	382	–	1.13	3.25	5.49	2.24
6d$'$	316	392	–	1.15	3.16	5.51	2.35
6e$'$	305	415	–	1.12	2.99	5.48	2.49

[a] UV–vis absorption and PL emission maxima measured in DMAc (for polyamides) or NMP (for polyimides) (5 μg/mL) at room temperature.
[b] UV–vis absorption edge measured as thin solid-film.
[c] Oxidation half-wave potentials from cyclic voltammograms.
[d] Energy gap = $1240/\lambda_{abs, onset}$ of the polymer thin film.
[e] The HOMO energy levels were calculated from $E_{1/2}$ and were referenced to ferrocene (4.8 eV).
[f] LUMO = HOMO − E_g.

polyamides exhibited strong UV–vis absorption bands at 314–361 nm in DMAc solution, assignable to the π–π^* transition resulting from the triphenylamine moieties. Their PL spectra in DMAc solution showed emission peaks around 421–430 nm in the blue region. The DMAc solutions of the polyamides were pale yellow and exhibited a medium blue PL under irradiation with long UV light (365 nm). Figure 3 shows the UV–vis absorption and PL spectra of triphenylamine-based diamine monomers and some typical polyamides **4a**, **4a$'$**, **4c**, and **4c$'$**. The absorption spectra of the polyamides in the solid state are similar (a little red-shifted) to those in DMAc solution. Optical band gap (E_g) determined from the absorption edge of the solid-state spectra of polyamides are found to be 2.86–3.15 eV. The PL spectra of these polyamides in the solid state are almost identical to those in dilute DMAc solution. Charge transport in organic materials is believed to be governed by the hopping process involving redox reaction of charge transport molecules. The redox behavior was investigated with cyclic voltammetry for the cast film on an ITO-coated glass substrate as working electrode in dry acetonitrile containing 0.1 M of tetrabutylammonium perchlorate (TBAP) as an electrolyte. The anodic scan provides information about ionization processes so that the highest occupied molecular orbital (HOMO) energy can be calculated. One reversible redox wave was observed in these polyamides. Figure 4 shows the typical cyclic voltammograns of the representative polyamides **4d** and **4d$'$** recorded at scanning rate of 100 mV/s. As depicted in Figure 4, scanning in a range from 0 to 1.2 V versus Ag/AgCl showed redox peaks with color changes. The polyamide **4d** showed an oxidation wave of which a peak top is at around 1.0 V. The electron removal for polyamide **4d** is assumed to occur at the nitrogen atom of the triphenylamine segments, which is electron-richer than the amide nitrogen atoms. The color of the film changed from pale yellow to green because of electrochemical oxidation of the polymer. The energy levels of the HOMO and LUMO of the investigated polyamides can be determined from the oxidation half-wave potentials ($E_{1/2}$) and the onset absorption wavelength, and the results are listed in Table 4. The external ferrocene/ferrocenium (Fc/Fc$^+$) redox standard $E_{1/2}$ is 0.44 V versus
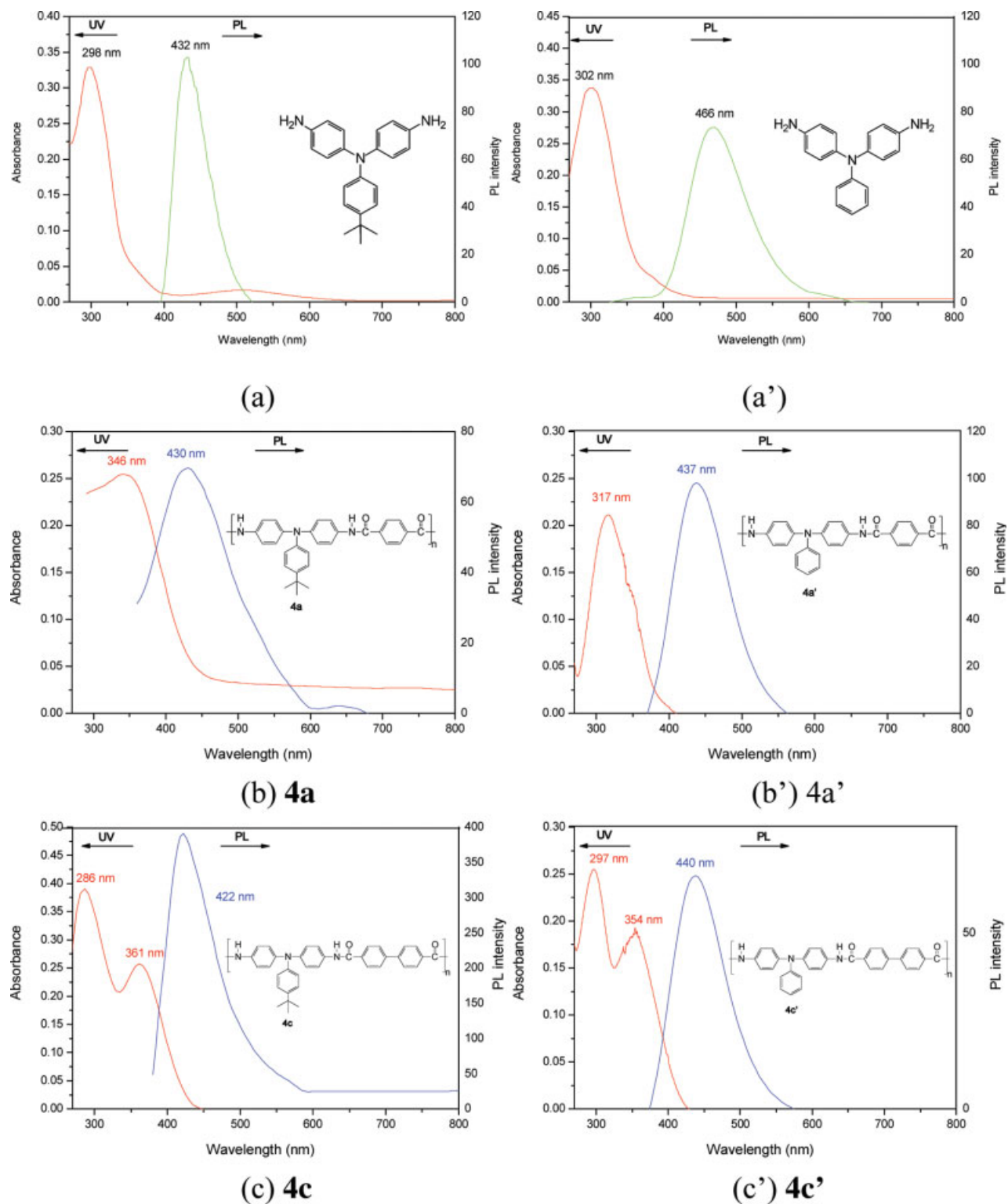
Figure 3. UV–vis absorption and PL spectra of triphenylamine-based diamine mono-mers and polyamides **4a**, **4a′**, **4c**, and **4c′** with a concentration of 5 μg/mL in DMAc. The insets show photographs of their solutions in DMAc emitting blue light when illumi-nated with a UV lamp. [Color figure can be viewed in the online issue, which is avail-able at www.interscience.wiley.com.]
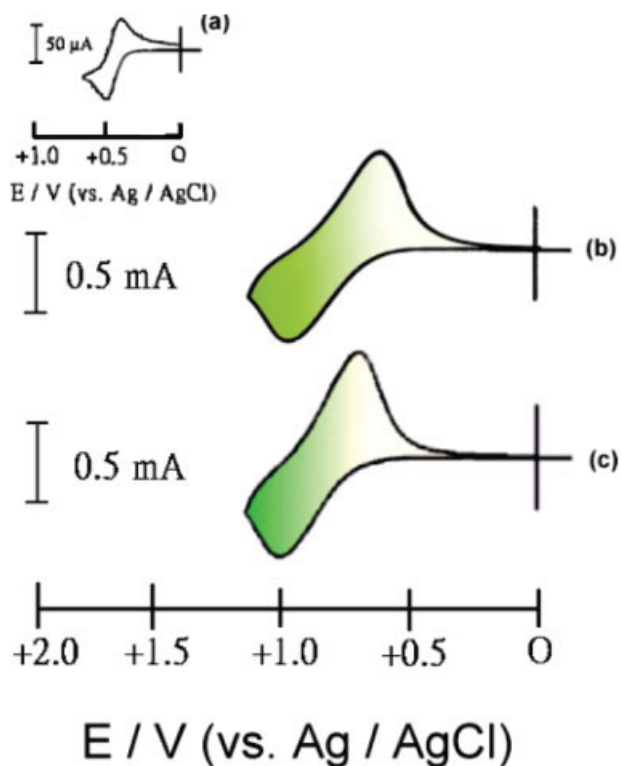
Figure 4. Cyclic voltammograms of (a) ferrocene, (b) polyamide **4d**, and (c) polyamide **4d′** as measured in 0.1 M TBAP/acetonitrile at a sweep rate of 100 mV/s. [Color figure can be viewed in the online issue, which is available at www.interscience.wiley.com.]

Ag/AgCl in acetonitrile. The HOMO value for the standard Fc is 4.80 eV with respect to the zero vacuum energy level. Therefore, the HOMO energy for polyamide **4d** has been evaluated to be 5.18 eV. With use of the same method, the HOMO positions of other polyamides were determined to be in the range of 5.17–5.21 eV. As compared with the corresponding structurally similar **4′** series polyamides, the **4** series polymers revealed a slightly lower oxidation potential and a higher HOMO level because of the incorporation of the *tert*-butyl group at the para position of triphenylamine moiety.

Polyimides **6c–6f** present similar spectra in NMP solutions and in the solid state, with λ_{max} at 304–319 nm. They exhibited significantly less detectable fluorescence than the polyamides. We propose that the observed quenching of PL that occurs in these polyimides is due to photoinduced electron transfer from donor triphenylamine to acceptor imide segment. Figure 5 shows the cyclic voltammograns of polyimides **6e** and **6e′** recorded at scanning rate of 100 mV/s; they showed an oxidation wave of which a peak top is around 1.15 V

(versus Ag/AgCl), with a color change from pale yellow neutral state to the blue oxidized form. The $E_{1/2}$ values of polyimides **6c–6f** were recorded in the range 1.08–1.13 V, which are higher than those of the polyamides because of the stronger electron-withdrawing nature of the imide group. Their HOMO energy levels were determined to be 5.45–5.49 eV (Table 4).

Spectroelectrochemical and Electrochromic Properties

The spectroelectrochemical properties of the polymer thin films were monitored by a UV–vis spectrometer at different applied potentials. The electrode preparations and solution conditions were identical to those used in cyclic voltammetry. The
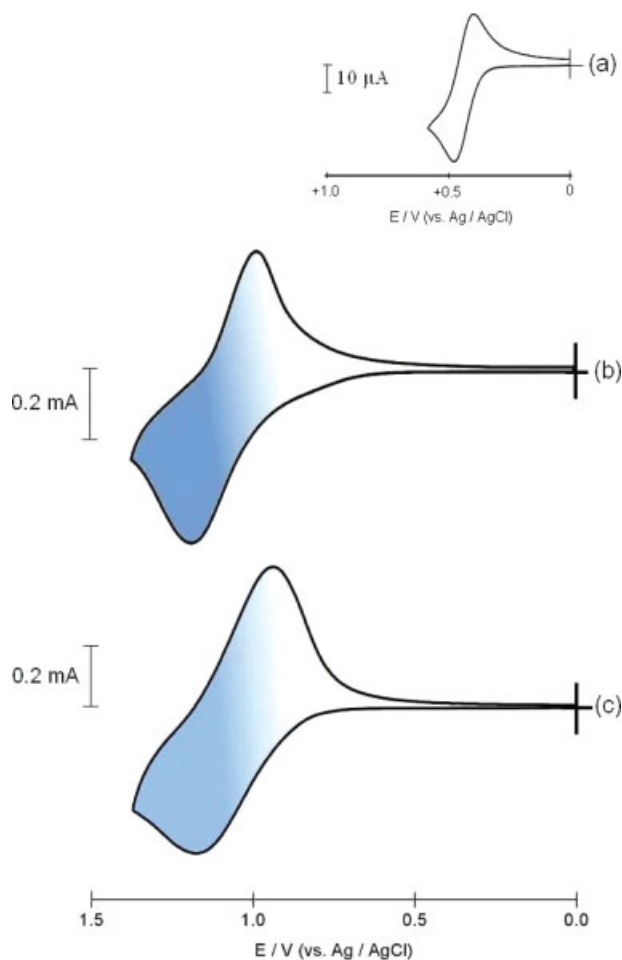
Figure 5. Cyclic voltammograms of (a) ferrocene, (b) polyimide **6e**, and (c) polyimide **6e′** as measured in 0.1 M TBAP/acetonitrile at a sweep rate of 100 mV/s. [Color figure can be viewed in the online issue, which is available at www.interscience.wiley.com.]
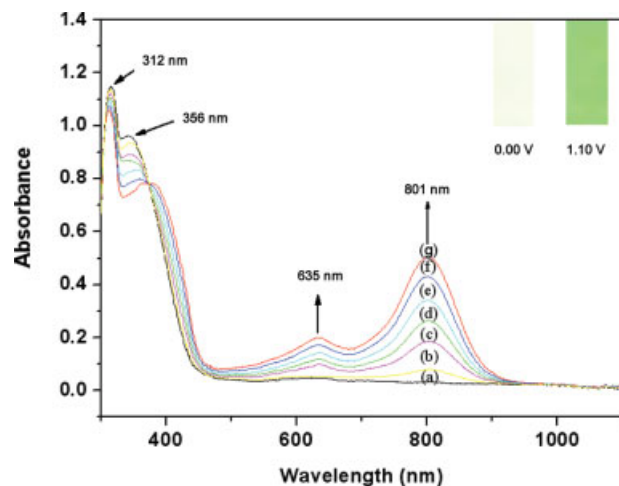
Figure 6. Spectroelectrochemical series of thin film of polyamide **4f** in 0.1 M TBAP/acetonitrile at various applied potentials: (a) 0, (b) 0.69, (c) 0.77, (d) 0.85, (e) 0.93, (f) 1.01, and (g) 1.10 V.

typical absorption spectral changes of polyamide **4f** are shown in Figure 6. When the applied potential was increased positively from 0 to 1.10 V, the peak of characteristic absorbance at 356 nm for polyamide **4f** decreased gradually while two new bands grew up at 635 and 801 nm because of the electron oxidation. The new spectrum was assigned as that of the stable cationic radical of the polyamide, and the film color turned into the green as shown in Figure 6. The spectroelectrochemistry characteristics of polyimide **6e** are depicted in Figure 7. As the applied potential
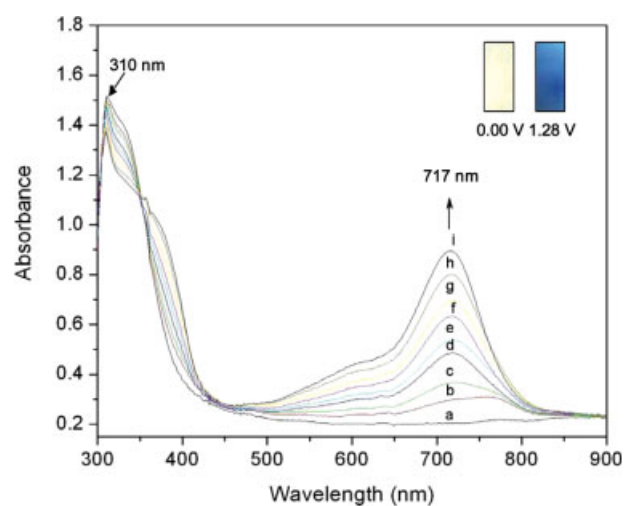
Figure 7. Spectroelectrochemical series of polyimide **6e** thin film in 0.1 M TBAP/acetonitrile at various applied potentials: (a) 0.00, (b) 0.80, (c) 0.87, (d) 0.94, (e) 1.01, (f) 1.08, (g) 1.15, (h) 1.22, and (i) 1.28 V.
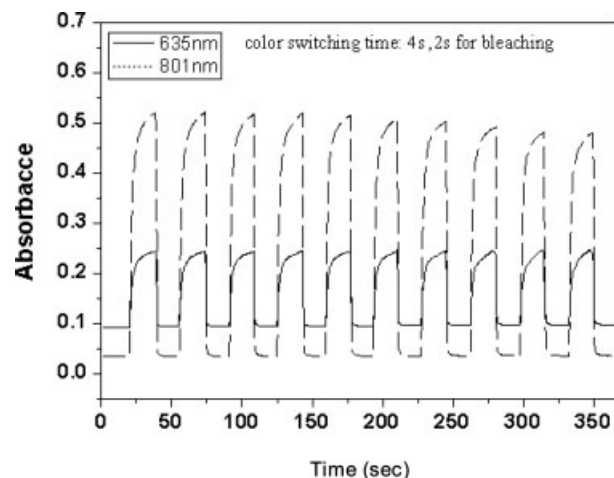
Figure 8. Potential step absorptometry of polyamide **4f** (in acetonitrile with 0.1 M TBAP as the supporting electrolyte) by applying a potential step (0 V $\leftrightarrows$ 1.10 V).

increased, the polymer started to get oxidized, and a decrease in the intensity of absorption at 310 nm was observed, one new band grew up at 717 nm because of the electron oxidation. The new spectrum was assigned as that of the radical cation of polyimide **6e**. Meanwhile the film color turned into the blue, as shown in Figure 7. The color switching times were estimated by applying a potential step, and the absorbance profiles were followed. The switching time was defined as the time that was required to reach 90% of the full change in absorbance after switching potential. Thin films from polyamide **4f** would require 4 s at 1.10 V for switching absorbance at 635 and 801 nm and 2 s for bleaching (Fig. 8). Continuous 10 cyclic scans between 0.0 and 1.10 V, the polymer films still exhibited excellent stability of electrochromic characteristics.

CONCLUSIONS

Several novel aromatic polyamides and polyimides with moderate to high inherent viscosities were prepared from a newly synthesized diamine monomer, 4,4′-diamino-4″-*tert*-butyltriphenylamine, with various aromatic dicarboxylic acids and dianhydrides, respectively. Incorporation of bulky and inherently electron-donating triphenylamine units to the polymer main chain and *tert*-butyl as pendent group not only functionalizes the polyamides and polyimides with stable redox properties but also leads to good solubility and excellent thin-film form-

ing ability associated with these polymers. In addition to high T_g or T_s values, good thermal stability, and mechanical properties, all the obtained polymers also revealed excellent stability of electrochromic characteristics by the electrochemical and spectroelectrochemical methods, changing color from the original pale yellowish to blue or green. Thus, these novel triphenylamine-containing polymers may find applications in electroluminscent devices as hole-transporting layer and electrochromic materials because of their proper HOMO values, excellent electrochemical and thermal stability.

REFERENCES AND NOTES

1. Yang, H. H. Aromatic High-Strength Fibers; Wiley: New York, 1989.
2. Polyimides; Wilson, D.; Stenzenberger, H. D.; Hergenrother, P. M., Eds.; Blackie: Glasgow, 1990.
3. Sroog, C. E. Prog Polym Sci 1991, 16, 561.
4. Polyimides: Fundamentals and Applications; Ghosh, M. M.; Mittal, K. L., Eds.; Marcel Dekker: New York, 1996.
5. Imai, Y. High Perform Polym 1995, 7, 337.
6. Imai, Y. React Funct Polym 1996, 30, 3.
7. Huang, S. J.; Hoyt, A. E. TRIP 1995, 3, 262.
8. De Abajo, J.; De la Campa, J. G. Adv Polym Sci 1999, 140, 23.
9. Eastmond, G. C.; Gibas, M.; Paprotny, J. Eur Polym J 1999, 35, 2097.
10. Li, F.; Fang, S.; Ge, J. J.; Honigfort, P. S.; Chen, J.-C.; Harris, F. W.; Cheng, S. Z. D. Polymer 1999, 40, 4571.
11. Li, F.; Fang, S.; Ge, J. J.; Honigfort, P. S.; Chen, J.-C.; Harris, F. W.; Cheng, S. Z. D. Polymer 1999, 40, 4987.
12. Chou, C.-H.; Reddy, D. S.; Shu, C.-F. J Polym Sci Part A: Polym Chem 2002, 40, 3615.
13. Wu, S.-C.; Shu, C.-F. J Polym Sci Part A: Polym Chem 2003, 41, 1160.
14. Hsiao, S.-H.; Chang, Y.-H. J Polym Sci Part A: Polym Chem 2004, 42, 1225.
15. Hsiao, S.-H.; Chang, Y.-M. J Polym Sci Part A: Polym Chem 2004, 42, 4056.
16. Liaw, D.-J.; Chang, F.-C. J Polym Sci Part A: Polym Chem 2004, 42, 5766.
17. Yang, C.-P.; Su, Y.-Y.; Wu, K.-L. J Polym Sci Part A: Polym Chem 2004, 42, 5424.
18. Hsiao, S.-H.; Chung, C.-L.; Lee, M.-L. J Polym Sci Part A: Polym Chem 2004, 42, 1008.
19. Yang, C.-P.; Su, Y.-Y. J Polym Sci Part A: Polym Chem 2004, 42, 222.
20. Liu, B.; Hu, W.; Matsumoto, T.; Jiang, Z.; Ando, S. J Polym Sci Part A: Polym Chem 2005, 43, 3018.
21. Liaw, D.-J. J Polym Sci Part A: Polym Chem 2005, 43, 4559.
22. Oishi, Y.; Takado, H.; Yoneyama, M.; Kakimoto, M.; Imai, Y. J Polym Sci Part A: Polym Chem 1990, 28, 1763.
23. Oishi, Y.; Ishida, M.; Kakimoto, M.; Imai, Y.; Kurosaki, T. J Polym Sci Part A: Polym Chem 1992, 30, 1027.
24. Liou, G.-S.; Hsiao, S.-H.; Ishida, M.; Kakimoto, M.; Imai, Y. J Polym Sci Part A: Polym Chem 2002, 40, 2810.
25. Liou, G.-S.; Hsiao, S.-H.; Ishida, M.; Kakimoto, M.; Imai, Y. J Polym Sci Part A: Polym Chem 2002, 40, 3815.
26. Liou, G.-S.; Hsiao, S.-H. J Polym Sci Part A: Polym Chem 2003, 41, 94.
27. Hsiao, S.-H.; Chen, C.-W.; Liou, G.-S. J Polym Sci Part A: Polym Chem 2004, 42, 3302.
28. Cheng, S.-H.; Hsiao, S.-H.; Su, T.-H.; Liou, G.-S. Macromolecules 2005, 38, 307.
29. Su, T.-H.; Hsiao, S.-H.; Liou, G.-S. J Polym Sci Part A: Polym Chem 2005, 43, 2085.
30. Liou, G.-S.; Hsiao, S.-H; Su, T.-H. J Mater Chem 2005, 15, 1812.
31. Liou, G.-S.; Hsiao, S.-H.; Su, T.-H. J Polym Sci Part A: Polym Chem 2005, 43, 3245.
32. Seo, E. T.; Nelson, R. F.; Fritsch, J. M.; Marcoux, L. S.; Leedy, D. W.; Adams, R. N. J Am Chem Soc 1966, 88, 3498.
33. Hagopian, L.; Kohler, G.; Walter, R. I. J Phys Chem 1967, 71, 2290.
34. Ito, A.; Ino, H.; Tanaka, K.; Kanemoto, K.; Kato, T. J Org Chem 2002, 67, 491.
35. Yamazaki, N.; Matsumoto, M.; Higashi, F. J Polym Sci Polym Chem Ed 1975, 13, 1373.